THE JOURNAL OF PHYSICAL CHEMISTRY B

Feature Article

pubs.acs.org/JPCB

Role of Proteome Physical Chemistry in Cell Behavior

Kingshuk Ghosh,*[,†] Adam M. R. de Graff,[‡] Lucas Sawle,[†] and Ken A. Dill*[,‡]

[†]Department of Physics and Astronomy, University of Denver, Denver, Colorado 80209, United States

[‡]Laufer Center for Physical and Quantitative Biology and Departments of Chemistry and Physics and Astronomy, Stony Brook University, Stony Brook, New York 11794, United States

ABSTRACT: We review how major cell behaviors, such as bacterial growth laws, are derived from the physical chemistry of the cell's proteins. On one hand, cell actions depend on the individual biological functionalities of their many genes and proteins. On the other hand, the common physics among proteins can be as important as the unique biology that distinguishes them. For example, bacterial growth rates depend strongly on temperature. This dependence can be explained by the folding stabilities across a cell's proteome. Such modeling explains how thermophilic and mesophilic organisms differ, and how oxidative damage of highly charged proteins can lead to unfolding and aggregation in aging cells. Cells have characteristic time scales. For example, *E. coli* can duplicate as fast as 2−3 times per hour. These time scales can be explained by protein dynamics (the rates of synthesis and degradation, folding, and diffusional transport). It rationalizes how bacterial growth is slowed down by added salt. In the same way that the behaviors of inanimate materials can be expressed in terms of the statistical distributions of atoms and molecules, some cell behaviors can be expressed in terms of distributions of protein properties, giving insights into the microscopic basis of growth laws in simple cells.

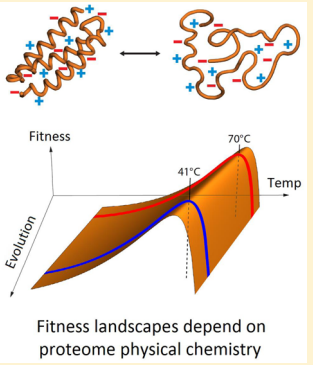

Fitness landscapes depend on proteome physical chemistry

CELLULAR GROWTH LAWS ARE RELATED TO CELLULAR FITNESS

Consider the simplest cells, such as bacteria or yeast. Cells grow at different rates, depending on their environment. A cell's growth rate depends on how much food is present, on the temperature and salt concentration of the external medium, and on its internal biochemical health. Because a cell's duplication speed is often the single most important determinant of its ability to propagate its progeny, growth rate could have evolved to be a complicated function of many biochemical details of a cell. However, we review here recent efforts toward a different view. Modeling shows how the growth laws of simple cells are encoded within the physical properties of a cell's *proteome* (i.e., its full complement of proteins). That is, some cell behaviors are attributable to large fractions of the proteome, not just a single protein or gene or pathway. And, some behaviors are physical (due to protein folding, aggregation, or diffusion, applicable in some universal or general way across different proteins), rather than biological (due to the protein's particular biological action). Of course, at best, simple models of the physical proteome are only a first approximation. But, in the spirit of other physical chemistry, they may provide useful conceptual insights and can make testable predictions.

First, we make a general point: growth laws are related to, and manifestations of, evolutionary fitness landscapes. Define a cellular growth rate, λ, as the number of new cells produced per unit time from each existing parent. If $c(t)$ is the cell population at time t, then under appropriate conditions, populations grow as

$$\frac{dc}{dt} = \lambda c \tag{1}$$

The growth rate λ can depend, often strongly, on various quantities; these are called *growth laws*. Perhaps the best known growth law,[1] $\lambda = \lambda(\text{sugar})$, indicates that cells grow faster with increasing concentrations of food, such as sugar, up to a point at which the growth rate saturates. Bacterial growth rates also depend strongly on temperature and external salt concentrations. For practical bacteriology, these are important. To kill bacteria, you remove a food source, or you heat the cells to high temperatures (as when you cook food), or you introduce high external salt concentrations (in pickling fish or in making jerky or salting meats, for example). In general, such growth laws can be expressed as $\lambda = \lambda(\mathbf{e})$, where $\mathbf{e}$ indicates a vector of *environmental* variables, such as sugar, temperature, or salt. These functions can express cellular growth laws.

A growth law is a function that describes how "today's cell" can respond to variations in today's conditions. But, cells can change those functions, through evolutionary modifications over longer time scales. This can be expressed in terms of their *genotype*, a vector of genes, $\mathbf{g}$. We use the term genotype here in a very general way: It can describe either a set of discrete options, such as the presence or absence of genes or amino acids in proteins, or a continuum of options. It can express some property of a gene directly or it can be a surrogate for that, representing some rate coefficients or equilibrium constants in the biochemical workings of the cell. In general, we can express the growth rate of a cell as

$$\lambda = \lambda(\mathbf{e}, \mathbf{g}) \tag{2}$$

Received: May 13, 2016
Revised: July 28, 2016
Published: August 11, 2016

DOI: 10.1021/acs.jpcb.6b04886
J. Phys. Chem. B 2016, 120, 9549−9563

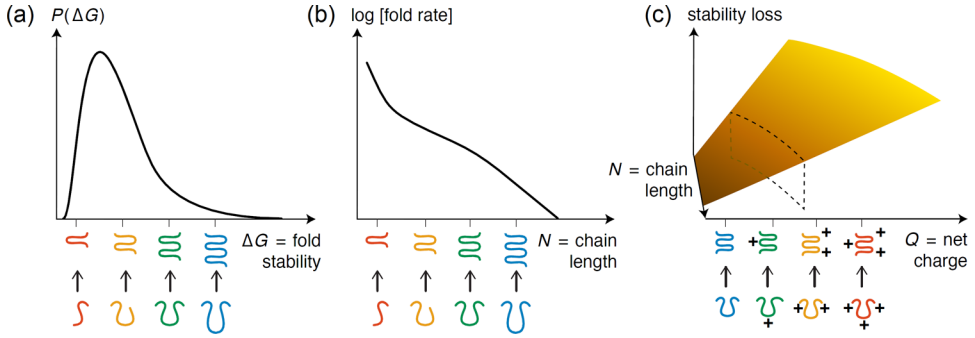

Figure 1. (a) Folding stability (ΔG) varies across a proteome, with longer proteins tending to have higher stability. (b) Mean folding rate decreases with increasing protein size (N). (c) Stability loss from a single side-chain charge modification (for example from oxidative damage) scales linearly with the net charge (Q) of the protein and affects small proteins more greatly than large proteins. While two-thirds of the human proteome lies within one standard deviation of neutrality (left of dotted boundary), and is relatively robust to charge modification, the high-charge outliers are at risk of large stability loss.

Equation 2 captures both today's growth law $\lambda = \lambda(\mathbf{e})$, for fixed evolutionary properties $\mathbf{g}$, while it also captures that growth rates can be modulated by evolution $\lambda = \lambda(\mathbf{g})$ for fixed conditions $\mathbf{e}$. The latter property, $\lambda = \lambda(\mathbf{g})$, is the *fitness landscape* for cells for which duplication speed is their primary measure of fitness. Hence, eq 2 relates, albeit in only a general abstract way, the evolutionary fitness landscape to the growth laws of cells. For cells that have been under a fixed selection pressure for a long time, and have evolved to maximize their fitness, we can study their peak-fitness points by finding

$$\left.\frac{d\lambda}{dg}\right|_{g*} = 0 \tag{3}$$

Note that, in general, cellular fitness f is not always equal to just λ, the growth rate. Many types of cells live in multicellular organisms. They contribute to the fitness of the whole organism. Their own particular fitness objectives are rarely known. Here, we describe some models of fitness $f(\mathbf{e}, \mathbf{g})$ in simple cells as a function of properties of the cell's proteins.

We focus on proteins because more than half of a cell's biomass is its proteins. Hence, where physical behaviors matter, proteins are likely to be predominant players. We distinguish between a protein's generic physicochemical properties and its specialized sequence-structure actions. By "general physical" properties, we mean the following. First, we are referring to a protein's health (also called *proteostasis*[2]): the balance between folded and unfolded states, the balance between folding and degradation, and the states of protein oxidation. Second, we are also referring to biophysical properties that can matter to the cell, such as protein movement, transport, crowding, sticking, and localization. Thanks to enzymatic assays, genome sequencing, and tens of thousands of atomically detailed protein structures in the Protein DataBank, the special functions of many proteins are now known. Less is known about the generic, physical, and health behaviors of proteomes. While the biological actions are often distinct from one protein to the next, the physical behaviors can involve *commonalities* among proteins, often arising more from statistical properties than from the singular native states. These properties include a proteome's distribution of stabilities, folding rates, and sensitivity to perturbations (such as side-chain charge modification), as shown in Figure 1. The physical properties of proteins are important because the cell commits major resources in energy and biomass toward managing them, in its struggle against stresses, disease, and death. Just like the specialized jobs of proteins, the generic actions can be changed through evolutionary processes such as natural selection.

Here, we describe how simple physicochemical models, combined with data from *in vitro* experiments, can predict some cell behaviors, rationalize observed growth laws, and generate hypotheses about diseases, aging, and evolutionary tendencies. The concepts being sought here, and the models being developed, are coarse-grained, not atomically detailed. Yet, despite their simplicity, they are often sufficient to generate testable hypotheses. The first example below shows how a coarse-grained model of protein folding stability can explain the high sensitivities of cells to temperature, rationalize thermal growth laws, predict proteome stability distribution functions, and give insight into how thermophilic organisms may have evolved to deal with higher environmental temperatures.

THERMAL PROPERTIES OF CELLS ARISE FROM THE FOLDING STABILITIES OF THEIR PROTEOMES

Cells are highly sensitive to temperature. It is not uncommon that the temperatures at which cells die are only a few degrees higher than the temperatures at which their growth is optimal.[3,4] Small shifts of environmental temperature can drive biological migrations, extinctions, genetic divergence, and speciation.[5−7] By what mechanism are cells so sensitive to temperature? Here, we review a polymer folding model (polymer-collapse theory) that indicates that the thermal sensitivities of cells arise because proteomes have evolved to have denaturation temperatures that are only marginally higher than the cell's growth temperature.[8−11] Despite its simplicity, this mechanism gives an approximate quantitative description of bacterial growth rates versus temperature.

Cells Are Sensitive to Temperature Because Their Proteomes Are Poised Near Their Denaturation Temperatures. This protein−denaturation−catastrophe mechanism[8,12] has been made quantitative by a combination of thermodynamic measurements of 59 mesophilic proteins *in vitro* with polymer-collapse theory. Such theory reckons that reversible protein folding is driven by the small average tendency of amino acids to prefer sticking to other amino acids inside a compact native structure, rather than to be exposed and solvated in an expanded unfolded state in water. This mechanism reckons that the principal force opposing folding is the chain entropy, which favors the unfolded state. A version of that simple idea also accounts for electrostatic interactions

DOI: 10.1021/acs.jpcb.6b04886
J. Phys. Chem. B 2016, 120, 9549−9563

and the effects of temperature, salts, and denaturants, giving the folding free-energy $\Delta G_{unfold} = G_{unfolded} - G_{folded}$ as[10,13,14]

$$\frac{\Delta G_{unfold}(T, \mathrm{pH}, c_s, c)}{kT_0} = -N\left[\frac{g_0 + m_1 c}{kT_0} + \frac{\Delta c_p}{kT_0}(T - T_h) + \frac{T}{T_0}\ln z - \frac{T}{T_0}\Delta c_p \ln\frac{T}{T_s} + \frac{l_b}{2N}\left(\frac{Q_n^2}{R_n(1+\kappa R_n)} - \frac{Q_d^2}{R_d(1+\kappa R_d)}\right)\right] \quad (4)$$

where g_0 represents the free-energy when amino acids desolvate and come into contact, z is the average conformational freedom loss per backbone bond, and Δc_p is the change in heat capacity per amino acid upon folding. Q_d and Q_n are the total net charge on the denatured and native structures, respectively, and R_d and R_n are the radii of denatured and native protein. N denotes the number of amino acids (or chain length) in the protein, c is the denaturant concentration, κ is the inverse Debye length, l_b is Bjerrum length, k is Boltzmann's constant, T is the temperature, $T_h = 373.5$, $T_s = 385$ K,[13,14] and $T_0 = 300$ K; for details, see refs 10 and 14.

Equation 4 gives the stability for a single average protein of length N. Thus, the probability distribution $p(\Delta G)$ of stabilities of all the proteins in a proteome (Figure 1a) can be computed from $P(N)$, the distribution of chain lengths of proteins in a cell.[8] $P(N)$ is available for different cell types from proteomic or genomic data.

We conclude that proteomes tend to be marginally stable at their physiological temperatures; see Figure 2. This marginal stability is not because the average stability is low, but because of the *distribution* of stabilities. The average protein in *E. coli* is estimated to be reasonably stable, $\Delta G_{unfold} = 6.8$ kcal/mol at 37 °C. However, there are many proteins that populate the "unstable" side of the distribution: approximately 550 out of 4300 (size of the *E. coli* proteome) proteins are less stable than 3 kcal/mol. In the absence of much data, we can estimate how stability is affected by protein domain structure,[15] and it indicates that proteins may be even less stable than the estimates above.[8] Furthermore, while these estimates are based on stabilities measured *in vitro*, experiments and simulations show that protein stabilities *in vivo* or in the reconstituted cytosol are comparable to, or even slightly less stable than, those *in vitro*.[16−20] The polymer folding model predicts that this marginally stable subset of the proteome is responsible for the high thermal sensitivity of the cell, as seen in Figure 2 by a small shift in temperature from 37 to 41 °C.

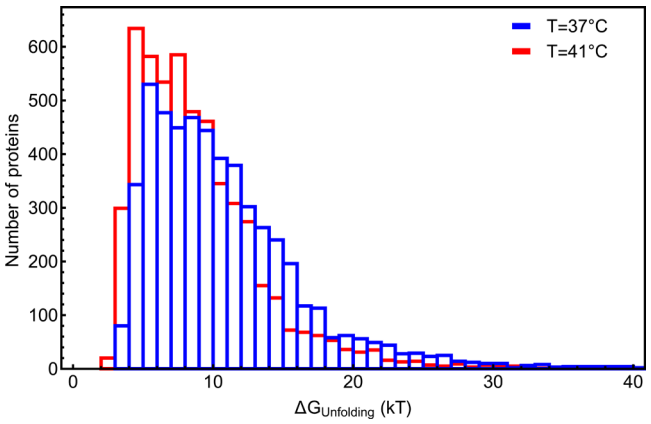

Figure 2. Distribution of unfolding free-energy ($\Delta G_{unfold} = G_{unfolded} - G_{folded}$) of all the proteins present in the *E. coli* proteome at 37 °C (in blue) and at 41 °C (in red). The bin width for the free-energy is 1 kT. The total area under the curve equals the number (4300) of proteins present in the *E. coli* proteome. Adapted with permission from ref 8. Copyright 2010 Elsevier.

A similar stability distribution is predicted by an evolutionary kinetics model.[9] In that treatment, random mutations occur through evolution that can alter the folding stabilities of proteins. Evolutionary changes occur by a random walk with a drift on the folding free-energy landscape.[9,21] That work envisions two limiting states. Proteins have a maximum stability, ΔG_{max}, because it becomes increasingly harder for evolution to find sequences having arbitrarily high stabilities. Proteins also have a minimum stability, ΔG_{min}, because otherwise they will aggregate or not fold. Within these two limits, it is assumed that the fitness landscape is flat. The protein stability distribution that evolves through this evolutionary model gives the same stability distribution as the polymer folding model.[8]

Both the polymer folding model and the evolutionary kinetics model give a basis for rationalizing the functional form of cellular thermal growth laws.[8,10−12] We suppose that the cell's growth rate, $r(T)$, is a product of two terms: (i) a factor that describes Arrhenius-activation of one or more activated metabolic process(es) that govern how the cell's growth rate increases with temperature at low temperatures,[8,12,22,23] and (ii) a factor that accounts for the fraction of the proteome that is folded at any temperature (capturing the denaturation catastrophe of the proteome at high temperatures[8,11,12]):

$$r(T) = r_0 \exp\left(\frac{-\Delta H^{\ddagger}}{kT}\right)\prod_{i=1}^{\Gamma}\frac{1}{1+\exp(-\Delta G_{unfold}(N_i, T)/RT)} \quad (5)$$

Here, r_0 is some reference growth rate, $\Delta H^{\ddagger}$ is the activation barrier of some critical growth-limited metabolic rate, and Γ is the number of essential proteins that are needed for growth. The product denotes multiplication over the probability that the ith essential protein (with N_i amino acids) is in the folded state which is written in terms of ΔG_{unfold} (eq 4; typical temperature dependence shown in Figure 3a). The expression above is simplified by assuming lethal proteins are drawn from the same distribution as the proteome,[8,12] thus enabling the calculation over all the proteins in the proteome, with Γ being a fit parameter. The details of the calculation can be found in previous work.[8,10] Similar arguments[22,24] have been made but using only a single effective value for ΔG_{unfold}. The model described here, based on the whole proteome stability distribution, fits well the experimentally measured growth rates for mesophilic organisms (Figure 3b). The corresponding best-fit value of the cell's activation barrier for growth, $\Delta H^{\ddagger}$, for *E. coli* is found to be 16.3 kcal/mol. This happens to be approximately equal to the barrier for peptide bond formation by the ribosome,[25] and is consistent with estimates from other studies.[12,22−24] Moreover, this activation energy is in the same range as typical values for various enzymatic reactions, including the barrier (13 kcal/mol) that is associated with the elongation of RNA by transcription.[26] This model also fits the growth rates of thermophilic organisms (Figure 3c) well when

DOI: 10.1021/acs.jpcb.6b04886
J. Phys. Chem. B 2016, 120, 9549−9563

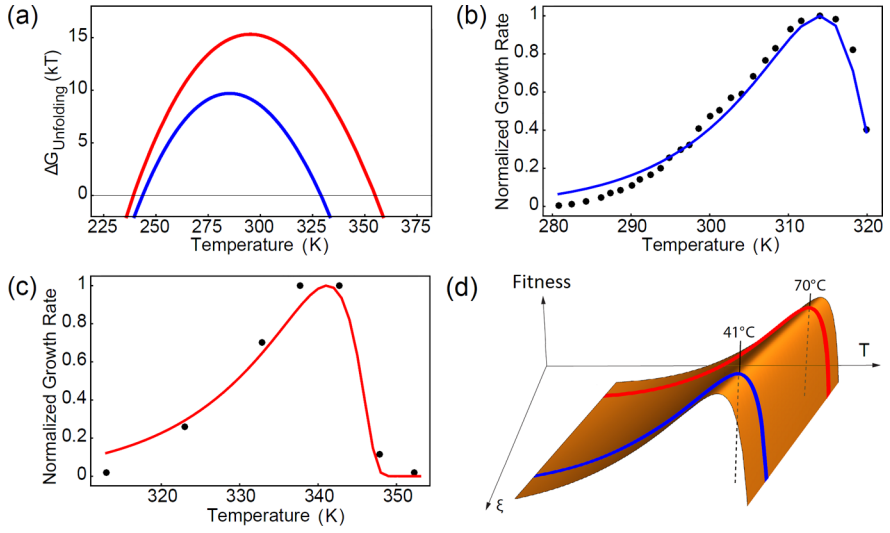

Figure 3. (a) Protein folding stability across temperatures (ΔG_{unfold}) for an ideal mesophilic (blue) and thermophilic (red) protein based on thermodynamic data.[10] (b) The growth rate model (blue) captures the experimental growth rate of mesophiles like *E. coli* (●) and (c) thermophiles (red).[10] (d) Temperature–growth curves in parts b and c can be seen as slices through a high-dimensional fitness landscape. Some dimensions can be traversed rapidly (like temperature), while others (ξ) change over evolutionary time scales. Reprinted in part with permission from ref 10. Copyright 2011 Elsevier.

using thermodynamic parameters for thermophilic proteins obtained from analyzing *in vitro* data sets.[10] A detailed systems level model has been applied to understand how mutations in metabolic networks change thermal growth rates.[27,28] They also indicate that the thermostabilities of metabolic enzymes are rate-limiting at superoptimal temperatures.[28] These models and arguments suggest that fundamental physicochemical properties of proteomes help to define a cell's evolutionary fitness landscape (Figure 3d).

Proteomes of Thermophilic Organisms Are More Stable Than Those of Mesophilic Organisms. The polymer-collapse model also gives insight into how mesophilic cells differ from thermophiles. *Mesophilic* organisms mostly live at moderate temperatures (25–40 °C) while *thermophilic* organisms grow at higher temperatures. How do their proteomes differ? A global analysis of 57 thermophilic proteins and 59 mesophilic proteins shows an average systematic difference:[10] thermophilic proteins denature at higher temperatures than mesophilic proteins, as they are more stable, on average, at all temperatures[10] (see Figure 3a). It also indicates that denatured states of thermophilic proteins may have less chain entropy than mesophilic proteins.[10] This implies that the denatured states are, on average, more compact in thermophiles;[29−31] see Figure 4. In principle, the difference in stabilities between thermophiles and mesophiles could arise from any of the types of driving forces, including electrostatics, hydrophobic interactions, proline substitution, disulfide bonds,[32−57] the presence of amino acids having different flexibilities,[58−61] or loop deletions.[62]

However, it seems likely that electrostatics may be a key contributor to these differences.[33−36,39−48,57,63,64] Electrostatic stability of folded proteins can depend both on a protein's net charge and on its charge patterning. For example, Sawle and Ghosh have shown that a good predictor of the relative compactness of the denatured structures between thermophilic and mesophilic sequences is the sequence–charge–decoration (SCD) metric:[57]

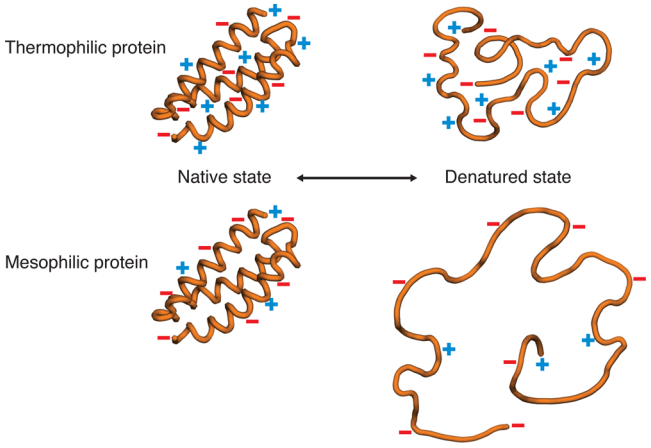

Figure 4. Denatured states are more compact in thermophilic proteins than in their mesophilic counterparts. Among other things, this can result from less net charge on thermophilic proteins or from more subtle differences in charge patterning (see ref 57 for details).

$$\mathrm{SCD} = \frac{1}{N}\left[\sum_{m=2}^{N}\sum_{n=1}^{m-1} q_m q_n (m-n)^{1/2}\right] \quad (6)$$

Here, q_n, q_m are the charges (1 for basic, −1 for acidic, and 0 otherwise) on two amino acids m and n with $|m-n|$ being their sequence separation. SCD expresses the degree of charge mixing;[57] a similar metric has been given by Das and Pappu.[65] Figure 5 gives the SCD values for two sequences of charge. A more compact denatured state is predicted by a more negative value of SCD. In this case, a "blockier" sequence of charges gives the more compact denatured state. Sawle and Ghosh have applied this metric to a set of 540 orthologous pairs of thermophilic and mesophilic proteins, and found that thermophiles, in general, have a more compact denatured state than mesophiles.[57] While this comparison was made without corresponding 3D protein structures, a comparison has also been made of a smaller set of 55 well-aligned mesophile–thermophile pairs, for which structures are known.[66] This too

DOI: 10.1021/acs.jpcb.6b04886
J. Phys. Chem. B 2016, 120, 9549−9563

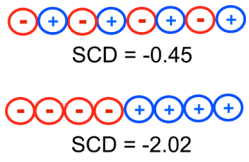

Figure 5. Sequence−charge−decoration (SCD) is a measure of charge patterning discrimination and a predictor of the compactness of a denatured state. The blockier sequence has the more negative SCD, predicting the more compact denatured state. A key distinction between mesophilic and thermophilic proteins appears to be the net charge and charge patterning of the protein sequences (see ref 57 for details).

shows that thermophilic domains are, on average and with high statistical significance, more compact than their mesophilic counterparts. Charge patterning and segregation also contribute to the sizes of intrinsically disordered proteins[65] and to the degree of ribosome−protein complexation.[67]

Highly Charged Proteins Are in Greater Danger of Unfolding from Random Oxidative Damage, Such as in Aging. Here is another way that protein folding stability appears to manifest as a phenotype of the cell. Cells sustain increasing oxidative damage with age.[68−71] Protein damage with age follows a fairly universal behavior, independent of organism (Figure 6). We describe here a hypothesis about how oxidative

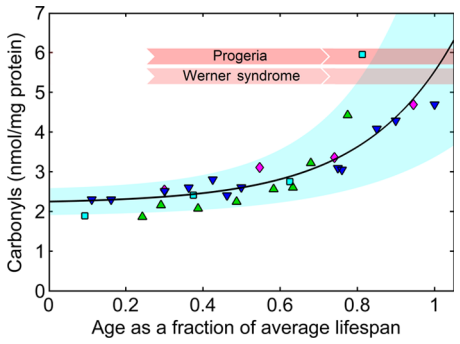

Figure 6. Diverse range of organisms share a common age-dependent increase of oxidative damage. The amount of protein damage with age is shown for worms[69] (purple ◆), flies[70] (green ▲), rats[68] (cyan ■), and humans[71] (blue ▼). The black curve is the fit to the data, while the blue shaded region is the range of curves obtained if the fit parameters are changed by 15%. The pink stripes show the damage levels reached at the end of life in people with the premature aging diseases progeria and Werner syndrome.[71] Reprinted with permission from ref 72. Copyright 2016 Elsevier.

damage can lower the folding stability of some of the proteome's proteins.[72] A few things are clear. First, proteins are key targets of oxidative damage.[73−75] As many as half of the proteins in an average 80-year-old person are estimated to have oxidative damage.[68,74] Second, amino acid side-chains are the principal site of damage,[75−78] estimated to be at least 10 times more common than other types of damage.[75] Third, oxidative damage is a random "loose cannon" event in the cell, hitting proteins across the spectrum of the whole proteome. So, random side-chain damage may be an important consequence of oxidation. But, one additional fact poses a challenge for modeling: the level of oxidative damage in old cells amounts to only about one amino acid alteration per protein,[68,74] a relatively small effect. How might single charge changes in some proteins be sufficient to contribute to the aging phenotype?

Here, we review the following mechanism:[72] (i) oxidation damages amino acid sites on random proteins across the proteome; (ii) some damage events will alter the charges on some side-chains;[77] (iii) for a small subset of the proteome, a small change in net charge (as small as +1 or −1 charges) can denature or destabilize its folded state. How can changing a protein's charge by only +1 or −1 units unfold a protein? Equation 4 contains an expression of electrostatic contribution to the free-energy of folding in terms of Q_n^2 and Q_d^2, the square of the charge on the native and denatured protein, respectively.[10,11] These terms capture the principle that it is unfavorable to bring a protein's net charge from the larger volume of the unfolded state to the smaller confines of the native state[79,80] (see Figure 7a). This model has been

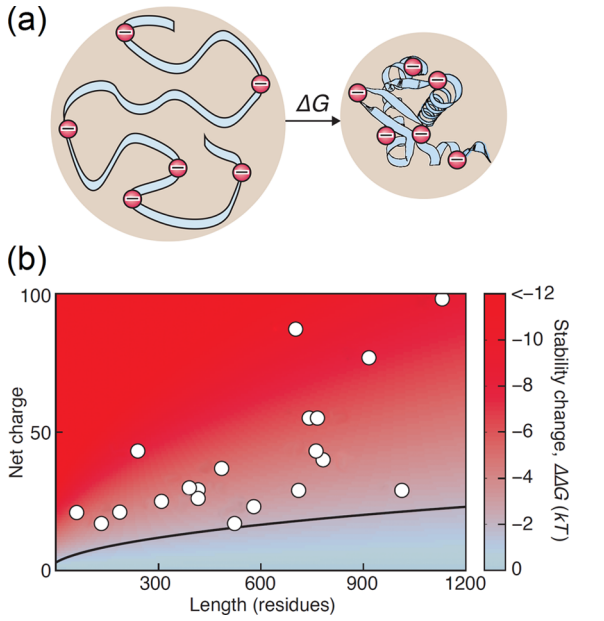

Figure 7. (a) For highly charged proteins, folding leads to the confinement of many charges into a small space. So, high net charge tends to destabilize the native fold. (b) This figure shows two points. First, the black line shows how one standard deviation of charge increases as a function of chain length in the human proteome. The color shading indicates the stability change predicted from a single destabilizing charge modification. The fact that the one standard deviation line coincides with the boundary between the blue and red regions indicates that most proteins in the human proteome are relatively long, neutral, and low-risk, yet there exists a significant number of outliers that are short, highly charged, and high-risk. Second, the points on this figure indicate 20 proteins that are important to aging and aging-related diseases and predicted to be in greater danger of large stability loss from a single oxidative charge modification. Some are among the most highly charged proteins in the proteome. Adapted with permission from ref 72. Copyright 2016 Elsevier.

demonstrated to predict the following: (i) the experimentally measured pH−salt phase diagrams for the unfolding of myoglobin, lysozyme, and RNase A,[14] and (ii) the experimental dependence of the folding free-energy on the square of the net charge.[79−82] Equation 4 shows that changing a protein's charge from Q to $Q \pm 1$, for example from a single oxidative damage event, will change an average protein's folding stability by $\Delta\Delta G(Q) = \Delta G(Q \pm 1) - \Delta G(Q)$, where

DOI: 10.1021/acs.jpcb.6b04886
J. Phys. Chem. B 2016, 120, 9549−9563

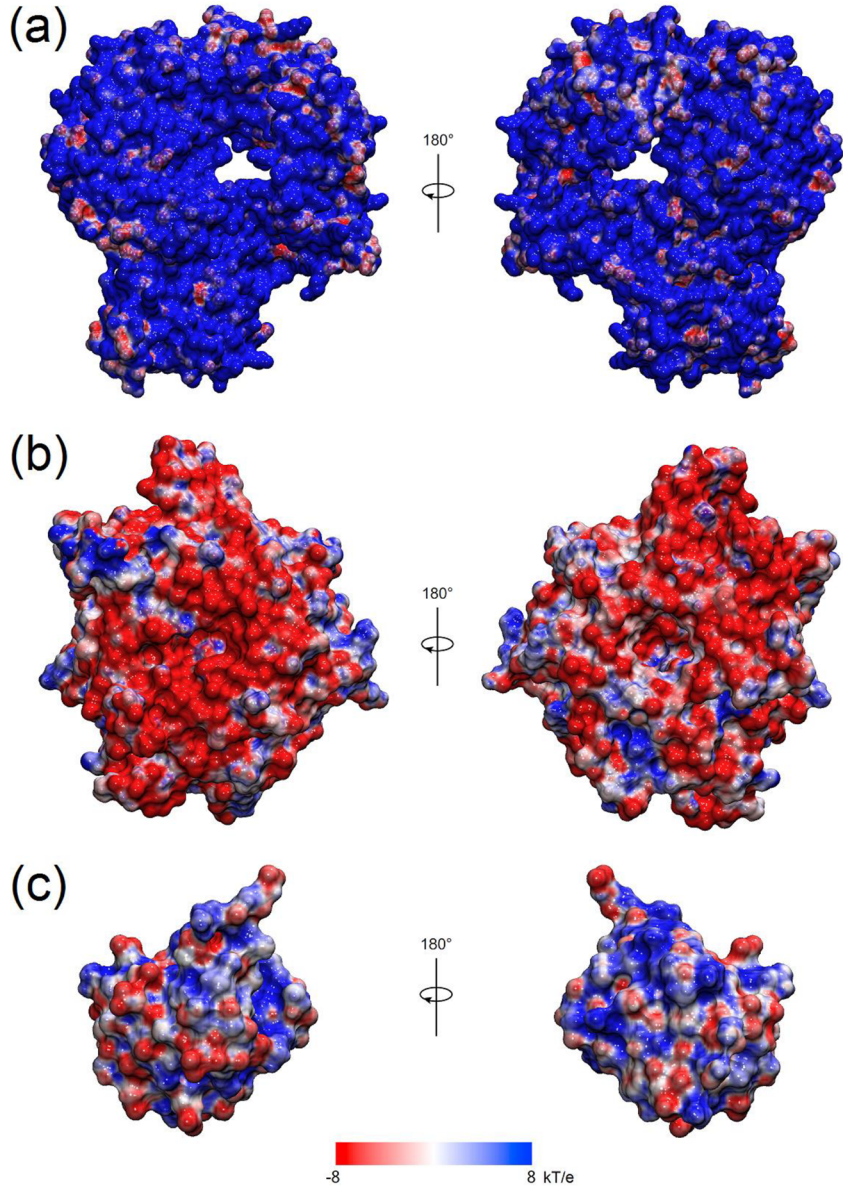

Figure 8. Electrostatic surface potential of (a) telomerase reverse transcriptase (1132 residues and +98 net charge in Figure 7b; PDB: 3KYL) and (b) nucleosome-remodeling factor subunit RbAp48 (425 residues and −29 net charge; PDB: 2XU7) are substantially different from the smaller, more speckled potential at the surface of (c) ubiquitin (76 residues and zero net charge; PDB: 1UBQ).[72] Reprinted with permission from ref 72. Copyright 2016 Elsevier.

$$\frac{\Delta\Delta G(Q)}{kT} = \frac{(\pm 2Q_d + 1)l_b}{2R_d(1 + \kappa R_d)} - \frac{(\pm 2Q_n + 1)l_b}{2R_n(1 + \kappa R_n)} \quad (7)$$

Equation 7 is in quantitative agreement with charge-perturbation experiments.[81,82] It can be computed using only a protein's sequence. It predicts a proteome-wide distribution of stability changes that is similar to that observed experimentally in point mutations of charged residues, which are reasonable proxies for oxidation.[83]

A key conclusion from eq 7 is that the change in folding free-energy, $\Delta\Delta G$, from a damage event will be proportional to the *net charge already on the native protein before the damage event*. So, any proteins in the proteome that are highly charged and/or relatively unstable to begin with are in greater danger of being destabilized by a single oxidative damage event; see Figure 7b.

Figure 7b shows an interesting implication of the model.[72] First, the black curve shows the one standard deviation line for the human proteome. It shows that most human proteins are sufficiently neutral to be safe from unfolding by single charge-modification events. Only a few of the proteins in the proteome have a sufficiently high net charge (of either sign) for the destabilization of their native state to be comparable to the stability of some entire proteins (roughly 2−4 kT; see Figure 2).

Now, notice the data points on Figure 7b. These are 20 human proteins known from the literature to be relevant to aging.[84] These 20 proteins all lie in the high-risk region, and thus, the model predicts that these proteins can be unfolded by a single oxidative charge-modification event. So, changing a single side-chain charge by a random oxidation event could contribute to how aging cells lose protein stability and function.[85] Figure 8 compares a typical charge distribution

DOI: 10.1021/acs.jpcb.6b04886
J. Phys. Chem. B 2016, 120, 9549−9563

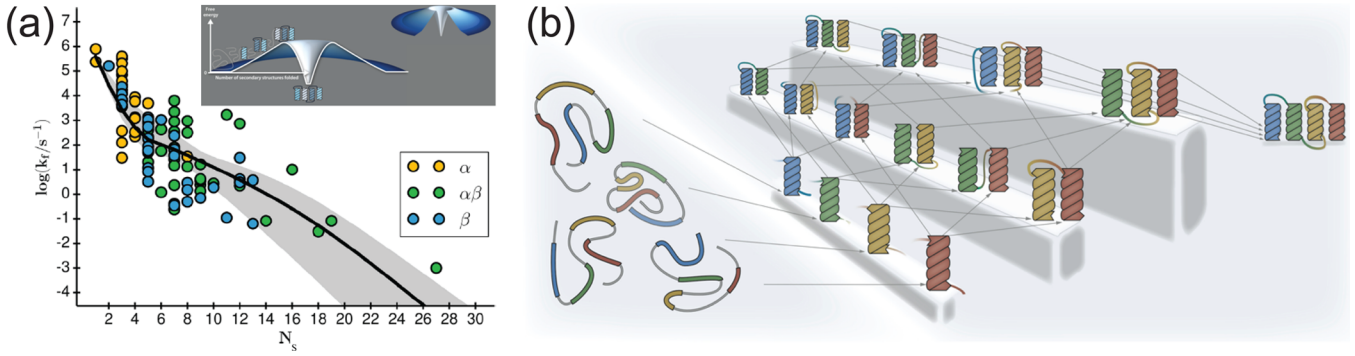

Figure 9. (a) Foldon Funnel Model predictions for protein folding rates vs number of secondary structure units (N_s), compared to data on 93 small single-domain proteins. The inset shows the funnel landscape for this model. (b) Mechanism for how local structures form first and then assemble toward the native state.[95] Reprinted with permission from ref 95. Copyright 2014 American Chemical Society.

found on the majority of proteins, which are nearly neutral (Figure 8c) and not at risk of unfolding from random oxidation events, with those of highly charged proteins (Figure 8a,b) at high risk of unfolding from single oxidation events.

Additional observations support this mechanism: high net charge is known to predict disorder-prone, unstable proteins;[86] disorder and low stability increase the chance of becoming oxidatively damaged;[87] protein aggregates of old organisms are enriched in damaged proteins;[88] and in budding yeast[89] and worms,[90,91] aggregates are known to be enriched in highly charged proteins such as ribosomal and DNA-binding proteins.[72] Interestingly, low net charge is also a signature of thermophilic proteins,[57] which face greater stability challenges, as discussed earlier.

DYNAMICAL PROPERTIES OF CELLS ARISE FROM THE FOLDING, SYNTHESIS, DEGRADATION, AND TRANSPORT RATES OF PROTEINS

Below, we review some of the time scales and dynamical processes of proteomes that are important to rapidly duplicating cells.

Protein Folding Happens Fast Enough To Escape the "Grim Reaper" of Proteome Degradation. First, consider the distribution of protein folding times. Experiments show that single-domain proteins fold *in vitro* over time scales that range over about 8 log orders.[11,92−96] Thirumalai developed an early model,[97] predicting that folding rates would scale as $k_f = k_0 \exp(-N^{1/2})$ with chain length N. It was remarkably prescient, given the almost complete absence of data at that time. It successfully describes folding rates of proteins[98] and RNA molecules.[99] Recently, a microscopic folding mechanism has been proposed, called the Foldon Funnel Model; see Figure 9. The model asserts a simple folding mechanism, namely, that local structures form first and rapidly, followed by larger nonlocal structures that assemble more slowly because they have to wait for smaller pieces to form first.[95] The model gives good predictions of folding rates for 93 single-domain proteins from sensible values of helix−coil and hydrophobic interaction parameters[95] (Figure 9a). The model predicts a median nonabundance-weighted folding time of 5 s for the *E. coli* proteome.[95]

Another model of folding rates is the Topology Polymer Model.[94] It treats the chain conformations more explicitly than the Foldon Funnel Model, fully accounting for entropic costs of chain topological restrictions (see polymer diagrams in ref 94 for details). The Topology Polymer Model also differs by (i) using structure-based domain assignments to predict folding rates and (ii) weighting the folding rates by protein abundance when predicting the proteome folding rate distribution.[96] The Topology Polymer Model gives good predictions for the dependence of folding speed on native topology[94,100] and unifies different models of folding kinetics. It predicts an average abundance-weighted folding time of 100 ms for the *E. coli* proteome, and it predicts an average of 170 ms for the yeast proteome.[96] The role of topological constraints in nucleic acids, proteins, and folding kinetics has also been recently revisited using simple folding models.[101,102] A question for the future remains: What are the folding rates of large single-domain or multidomain proteins? There are not yet many experiments for those types of proteins.[15,103]

Figure 10a compares the protein folding times for the yeast proteome (from the Topology Polymer Model) with other key rates in the cell.[96] The rate distribution is broad. The most remarkable prediction is that folding speeds seem nearly optimal for outrunning the "grim reaper" of protein degradation,[96] with the slowest-folding proteins just barely out-pacing the fastest protein degradation. This case is made by the black curve in Figure 10a, which is the result of an evolutionary diffusion-drift model of folding rates,[96] resembling the diffusion-drift model of protein stabilities[9] described earlier. The model is based on asserting two physical principles of evolution, namely, that (i) no protein can fold faster than known ultrafast folders, due to conformational speed limits,[105] and (ii) no protein should fold more slowly than the fastest degradation time. Within this interval, the only selection pressure on folding kinetics is simply to "beat the clock" against degradation.[96] When fitted with only one parameter against the folding time distribution derived from the Topology Polymer Model, the model predicts the slowest folding time to be around 10 s. This provides a cushion of an order of magnitude in time separation relative to the fastest degradation times (a few minutes). So, even a protein that degrades at the fastest rate, if not folded off the ribosome by cotranslational folding, has at least a 90% chance of folding before being degraded.[96] For yeast, almost 99% of the proteome's proteins fold faster than the degradation time (see Figure 10b and ref 96 for details). Among the four outliers, the only protein that folds significantly more slowly has 18 chaperone interaction partners,[96] indicating the important role of chaperones in helping slow folders.[106]

Speed of Cell Duplication Is Limited by the Rate of Protein Translation. What is the speed limit for cell

DOI: 10.1021/acs.jpcb.6b04886
J. Phys. Chem. B 2016, 120, 9549−9563

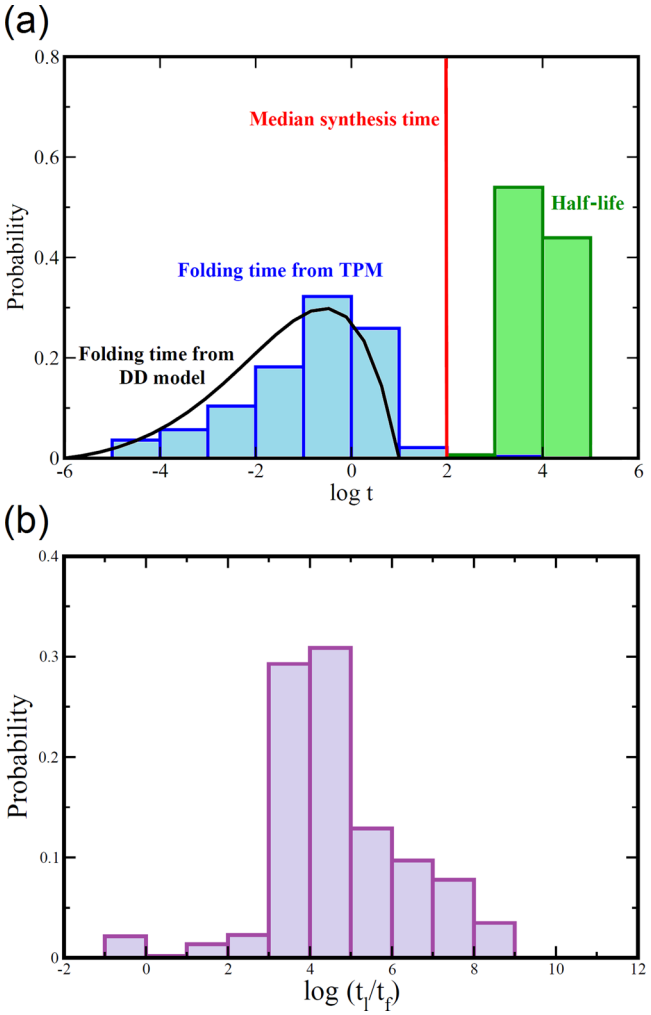

Figure 10. (a) Abundance-weighted folding time (t in seconds) distribution across the yeast proteome (blue) using the topology polymer model,[94] which is in good agreement with diffusion-drift model (black) with flat fitness landscape.[96] Experimentally measured half-life distribution of the yeast proteome (green)[104] shows folding kinetics is faster than protein degradation.[96] Median synthesis time is shown in red. (b) The distribution of the ratio of protein half-life and protein folding time.[96] Adapted with permission from ref 96. Copyright 2014 Zou et al.

duplication? In rapidly growing *E. coli* bacteria, DNA replication takes 1−2 ms/base,[107] RNA polymerase 10−40 ms/base,[108,109] and the ribosome 50 ms/amino acid.[110] The ribosome's slower rate of elongation, combined with its enormous size (since the ribosome itself needs to get copied) and the 10-fold greater cellular abundance of polymerized amino acids relative to nucleotides, makes protein translation the largest bottleneck to cellular growth. In fast-growing *E. coli*, about a third of the cell's dry weight is ribosome (including rRNA).[111,112]

What is the maximum rate of protein synthesis? First, cell duplication requires that each ribosome must make a copy of its own proteins. The fastest that a ribosome can copy itself is 6 min, assuming a ribosome's 7336 amino acids[113] are translated at a rate of 20 per second.[114] Second, each ribosome must duplicate a corresponding complement of other proteins too. At fast growth rates, an *E. coli* ribosome must make roughly three times its own mass of nonribosomal proteins.[111,115] These nearly 30 000 amino acids must be duplicated in series, one-amino-acid-at-a-time, by each ribosome, predicting a minimum doubling time of 24 min, which approximately equals the observed maximum rate in *E. coli*.[111]

Interestingly, this 1:3 ratio of ribosomal to nonribosomal proteins also appears to hold in budding yeast, a fast-growing eukaryote.[116] So, the minimum cell division time t_d can be estimated as

$$t_d = 4rL \tag{8}$$

where r is the rate that one ribosome adds one amino acid to a growing protein chain, and L is the number of amino acids in a ribosome. A ribosome of budding yeast contains 1.6-fold more amino acids than *E. coli*'s[113,117] and elongates proteins at half the latter's speed.[110,116] So, if protein translation is indeed the limiting factor in the rate of cell duplication, it implies a minimum doubling time of $2 \times 1.6 \times 24$ min = 77 min. This is close to experimental values.[118]

Protein Translation Speeds Are Limited by Diffusion and Binding. So, why can an amino acid not be added to a growing peptide chain in less than 50 ms in *E. coli*? Translation is known to require several actions:[119,120] (i) tRNA needs to diffuse to the ribosomal binding site; (ii) the tRNA must settle and bind in the appropriate orientation at this site, with proofreading to verify that it is the correct tRNA;[119] (iii) the peptide is chemically elongated. It is thought that the peptide elongation reaction (iii) is faster than the accommodation step, but this is still debated.[119] The rate of tRNA accommodation (ii) has been found experimentally to occur on the same time scale as translation (i) and thus could account for a non-negligible fraction of the total 50 ms. The translation step (i) depends on tRNA concentration. Evidence for its role in a diffusion bottleneck is that cellular tRNA concentrations are roughly the same as those needed to saturate ribosomal kinetics.[121] Furthermore, *E. coli* devotes a significant fraction of its dry weight to tRNA (up to 2%[121]) that could have been spent on more ribosomes, suggesting tRNA plays an important role in protein synthesis speed. Consistent with this, a tRNA diffusion model correctly accounts for the abundance of tRNA with growth rate.[121] In short, it appears that the physical processes of tRNA diffusion (i) and the binding and proofreading (ii) are limits to the speed of ribosomal translation.

Cellular Actions May Be Broadly Rate-Limited by Protein Motions. Of course, there are very many metabolic rates in the cell. Figure 11a summarizes a broad range of enzyme actions, indicating a predominant time scale around 10−1000 ms.[122] What limits their rates? Typical enzyme reactions are often parsed into the following steps:

$$\text{open} \rightarrow \text{bind} \rightarrow \text{chemical reaction step} \rightarrow \text{close} \tag{9}$$

Among these steps, the chemical reaction step itself is often fast. The rate of collision between proteins and small diffusing ligands is on the order of 10^8 M^{-1} s^{-1}, implying a time scale of 0.1 ms for typical ligand concentrations of 0.1 mM.[122] Hence, the rate-limiting steps for enzyme actions appear to be the other steps in eq 9; namely, the opening and closing, binding, product release steps.[123−127] These steps can be limited by protein dynamics. Evidence for this view comes from the close correspondence between catalytic rates and the rates of functional motions observed across many proteins, as shown in Figure 11b. However, enzymatic efficiency can be enhanced by other subtle mechanisms as well. For example, binding of allosteric effectors can induce fluctuations[128] and alter conformational landscape either by facilitating conformational

DOI: 10.1021/acs.jpcb.6b04886
J. Phys. Chem. B 2016, 120, 9549−9563

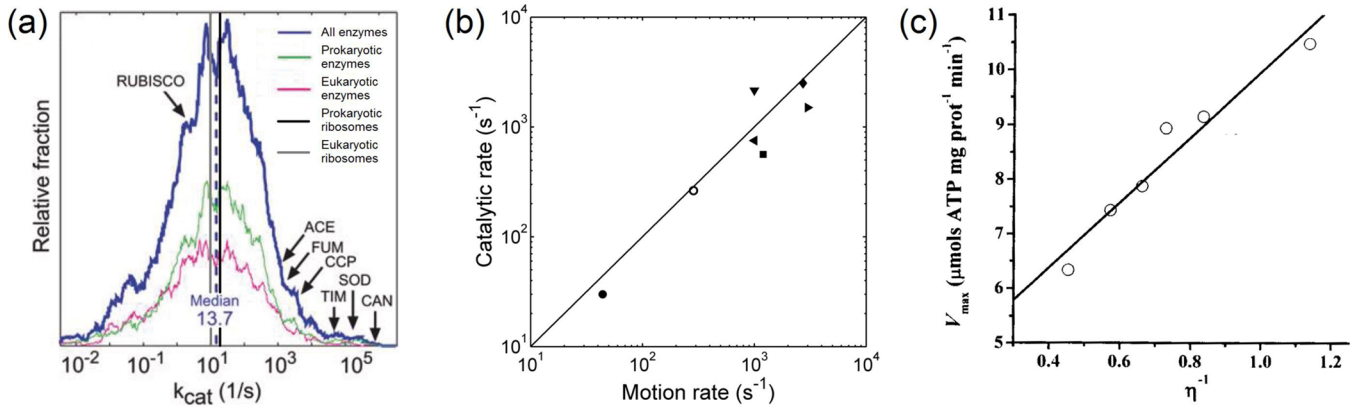

Figure 11. (a) Distribution of protein and ribosomal catalytic rates in prokaryotes and eukaryotes.[122] Ribosomal catalytic rates are remarkably similar to the proteome-wide averages. (b) Catalytic rates often closely follow those of the functional low-frequency motions of proteins. Mesophilic adenylate kinase (●),[123] thermophilic adenylate kinase (○),[123] T4 lysozyme (■),[133] triosephosphate isomerase (◀),[134] ribonuclease binase (▶),[135] RNase A (▼),[136] and cyclophilin A (◆).[137] (c) Enzyme catalysis slows down with increasing solvent viscosity in different concentrations of trehalose (○).[131] Part a adapted with permission from ref 122. Copyright 2011 Americal Chemical Society. Part c reprinted with permission from ref 131. Copyright 2004 Springer.

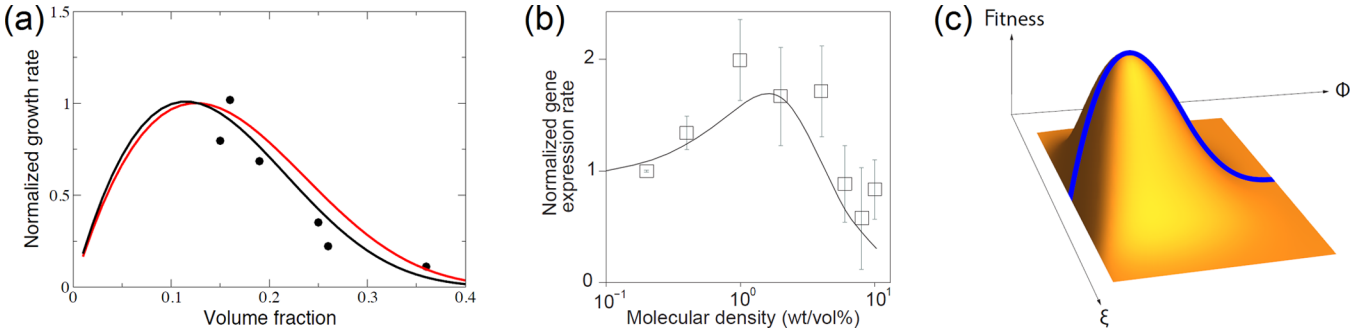

Figure 12. (a) Growth rate as a function of crowding volume fraction is well-captured by the hard-particle model of Minton.[148] (b) Cell crowding has similar consequences on the rate of gene expression.[149] (c) A high-dimensional fitness landscape (as a function of volume fraction (ϕ) and arbitrary reaction coordinate ξ) on which part a represents a single slice. Part b is reprinted with permission from ref 149. Copyright 2013 Macmillan Publishers Ltd.

transition or altering the width of the free-energy basin[129] and site-specific local flexibility.[130] Partitioning of flux between different pathways can also enhance turnover rates.[128] In spite of these subtleties, the overall role of protein dynamics in enzymatic turnover is clear (Figure 11b). Furthermore, enzyme actions often slow down with increased solvent viscosity[131] (Figure 11c). This is consistent with the observed effect of solvent viscosity on loop closure, which is rate-limiting for catalysis in some enzymes.[132]

So, if cell duplication speeds are ultimately limited by protein motions, why can proteins not wiggle any faster than they do? First, protein conformational energy landscapes are naturally rugged, even along directions of large-amplitude motions.[138] Second, large motions require moving against friction ("wet" friction of the solvent and "dry" friction from internal motions[139−142]). Third, some motions require local unfolding of secondary structures,[138] and that depends on protein folding stability, which is usually marginal.[127,138] Fourth, the protein conformation that binds the substrate is often little populated, and requires waiting for the right fluctuation. Lastly, there are trade-offs between high affinity for the substrate and stabilization of the transition state conformation.[127] In summary, the evidence compiled here indicates that cell duplication speeds are limited by ribosomal and enzyme actions, which are in turn limited typically by the diffusion of substrate and the motions of protein molecules as they slosh and contort in the solvent.

Salts Can Slow Down Cell Growth by Slowing the Rates of Movement of Proteins inside Cells. High salt concentrations can slow down the growth of bacteria. Salts are used to pickle foods and to preserve meats. Salts act by slowing down bacterial growth. Here, we describe a mechanism for bacterial salt growth laws: Adding external salt contributes an osmotic pressure that draws water out of the cell, causing the density of proteins inside the cell to increase, leading to more sluggish transport of the proteins throughout the cell's cytoplasm, and reducing the cell's growth rate. Experimental data shows a correlation between cellular growth rate and specific reactions such as translation speed[110,143] and other key metabolic reactions.[144] To obtain the salt growth law, we suppose that growth rates of cells are proportional to protein−protein collision rates (r_d) inside the cell, resulting from protein diffusional transport.

We hypothesize that biomolecular crowding has two opposing effects on reactions: (i) it increases the concentration of interacting species, but (ii) it hinders and slows the diffusion rate of the reactants. The combination of these two effects predicts a protein diffusional rate r_d that is proportional to $\phi D(\phi)$, where ϕ is the protein volume fraction and $D(\phi)$ is the diffusion constant depending on the crowding fraction. The

DOI: 10.1021/acs.jpcb.6b04886
J. Phys. Chem. B 2016, 120, 9549−9563

reduction of diffusion due to volume-excluding monodisperse hard-sphere crowders can be approximated by a simple formula: $D(\phi) \sim D_0 (1 - \phi/\phi_c)^2$, where D_0 is the diffusion in the limit of no crowding, and ϕ_c denotes the volume fraction at which diffusion critically slows down and is estimated to be $\phi_c \approx 0.58$.[11,145,146] The protein−protein collision rate is

$$r_d \sim \phi(1 - \phi/\phi_c)^2 \quad (10)$$

Maximizing r_d with respect to ϕ yields the optimal volume fraction of $\phi_{opt} \approx \phi_c/3 \approx 0.19$, close to the typical protein volume fraction (around 0.2) inside a cell.[11] We can compare this model's predictions to experiments on bacterial growth rate as a function of salt and crowding volume fraction.[147]

To account for heterogeneous protein sizes, two ingredients are needed. First, we have used the hard-particle theory of Minton,[148] and its parameters, to estimate how $D(\phi)$ varies with protein size. This model correctly captures the observed decrease in diffusion with increasing particle size.[148] Second, we need to know which particular protein or proteins are responsible for the diffusion limit to cell growth.

Figure 12a shows two different assumptions regarding which proteins are rate-limiting. First, the red curve supposes that all the proteins in the proteome participate in growth, taken by averaging the reaction flux over the molecular weight distribution of the whole *E. coli* proteome. Second, an argument has been made[143] that one particular type of biomolecule may have an outsized influence on cell dynamics, namely, the tRNA-EF-Tu complex, which are the 70 kDa particles that bring the tRNA molecules to the ribosome in order to elongate the growing peptide chain. As we have argued in the previous section, protein translation, which depends on the rates of amino acid incorporation, may be rate-limiting for cell growth. The basic translation speed of incorporating one amino acid at a time can be further slowed in the presence of crowding due to compromised diffusion. Might the diffusion of the tRNA-EF-Tu complex be growth-limiting? This is a large complex. It will diffuse slowly to the ribosome in the crowded cell environment. This diffusion-bottleneck hypothesis is supported by a recent study showing that ribosomes and tRNA are maintained close to the ratios predicted from diffusion arguments to optimize cell-wide translation rates.[143] The black curve in Figure 12 shows the model prediction when the diffusion of tRNA-EF-Tu complexes is considered to be rate-limiting.

Of course, other factors will matter too in the balance of salt and volumes of the cell, including ion fluxes, their regulation, and the balance of ATP.[150] The model described above only aims to give a simple estimate of the protein diffusional factor. Cellular crowding is known to affect many physiological processes.[151] Crowding can also affect gene expression levels (Figure 12b), reaching a maximum before decreasing at higher densities.[149,152] Recent work has also shown cytoplasm can exhibit glassy properties.[153,154] The nature of the cytoplasmic environment depends on the size of the cellular objects; for example, small objects experience cytoplasm as a liquid-background while large macromolecules experience a solid-like environment.[154] Interestingly, metabolism can also tune the fluidity of the cytoplasm allowing transport of large cellular components that will otherwise be severely constrained in their mobility. Thus, switching between different metabolic states under varying environmental conditions can alter dynamics, cell physiology, and ultimately cellular fitness.[154] Figure 12c shows how such relationships represent single slices through a high-dimensional fitness landscape that we are only beginning to understand.

SUMMARY

While many behaviors of cells emerge from their unique biology, they are fundamentally constrained by the common physics that unites them. Here, we review simple arguments about how these fundamental limits are encoded within the collective physical properties of proteins and proteomes. We describe the role of proteome physics in cell growth laws, providing mechanisms for how cell growth speeds up with temperature and how high salt concentrations slow it down. Electrostatics models give mechanistic insight into the stability gain in thermophiles and the oxidative stability loss in aging and disease. Furthermore, kinetic models of protein folding applied on a global scale show how folding times may be limited by the rate of degradation. And, we note that cell growth appears to be rate-limited by the ribosomal action of adding amino acids to growing protein chains, and by protein motions responsible for enzyme actions. In short, physics can give qualitative and quantitative insights into the growth properties of cells through the use of simple physical models. We believe such global scale models, guided by physicochemical principles, will be increasingly sought after to understand cellular phenotypes and evolution.

AUTHOR INFORMATION

Corresponding Authors

*E-mail: kghosh@du.edu. Phone: 303-871-4866.
*E-mail: dill@laufercenter.org. Phone: 631-632-5401.

Notes

The authors declare no competing financial interest.

Biographies

Kingshuk Ghosh earned his Ph.D. in Physics from the University of Massachusetts, Amherst, and received his Masters in Physics from the Indian Institute of Technology, Kanpur, and the University of Massachusetts, Amherst. He is currently an Associate Professor in the department of Physics and Astronomy at the University of Denver. His research interests include protein folding, modeling stochasticity in biochemical and genetic networks, principles of evolution, and foundations of statistical mechanics.

DOI: 10.1021/acs.jpcb.6b04886
J. Phys. Chem. B 2016, 120, 9549−9563

Adam de Graff earned his Ph.D. in Physics with emphasis in Biology from Arizona State University, and received a B.Sci. in Physics from the University of Manitoba. He is currently a Junior Fellow at the Laufer Center for Physical and Quantitative Biology at Stony Brook University. His research interests include protein stability, proteostasis, and the role of mitochondrial function and energy homeostasis in aging.

Lucas Sawle earned his Ph.D. in Physics from the University of Denver, and received B.Sci. degrees in Physics and Applied Mathematics from Indiana University South Bend. His research interests include enhanced protein thermal stability, protein folding, and computational simulation techniques.

Ken Dill received undergraduate degrees from MIT in Mechanical Engineering and a Ph.D. in Biology from the University of California, San Diego. He is the Director of the Laufer Center for Physical and Quantitative Biology and Distinguished Professor of Chemistry and of Physics and Astronomy at Stony Brook University. He is interested in the physical properties and evolution of proteins and cells.

■ ACKNOWLEDGMENTS

K.G. acknowledges support from the NSF (Award 1149992) and RCSA (Cottrell Scholar award); K.A.D. acknowledges support from the Laufer Center and NIH (R01GM063592-14).

■ REFERENCES

(1) Monod, J. The growth of bacterial cultures. *Annu. Rev. Microbiol.* **1949**, *3*, 371−394.
(2) Balch, W. E.; Morimoto, R. I.; Dillin, A.; Kelly, J. W. Adapting proteostasis for disease intervention. *Science* **2008**, *319*, 916−919.
(3) Lepock, J. Measurement of protein stability and protein denaturation in cells using differential scanning calorimetry. *Methods* **2005**, *35*, 117−125.
(4) Westra, A.; Dewey, W. Variation in sensitivity to heat-shock during cell-cycle of chinese hamster cells in-vitro. *Int. J. Radiat. Biol. Relat. Stud. Phys., Chem. Med.* **1971**, *19*, 467.
(5) Kennett, J.; Stott, L. Abrupt deep-sea warming, palaeoceanographic changes and benthic extinctions at the end of the Palaeocene. *Nature* **1991**, *353*, 225−229.
(6) Ivany, L.; Patterson, W.; Lohmann, K. Cooler winters as a possible cause of mass extinctions at the eocene/oligocene boundary. *Nature* **2000**, *407*, 887−890.
(7) Allen, A.; Gillooly, J.; Savage, M.; Brown, J. Kinetic effects of temperature on rates of genetic divergence and speciation. *Proc. Natl. Acad. Sci. U. S. A.* **2006**, *103*, 9130−9135.
(8) Ghosh, K.; Dill, K. Cellular proteomes have broad distributions of protein stability. *Biophys. J.* **2010**, *99*, 3996−4002.
(9) Zeldovich, K.; Chen, P.; Shakhnovich, E. Protein stability imposes limits on organism complexity and speed of molecular evolution. *Proc. Natl. Acad. Sci. U. S. A.* **2007**, *104*, 16152−16157.
(10) Sawle, L.; Ghosh, K. How do thermophilic proteins and proteomes withstand high temperature? *Biophys. J.* **2011**, *101*, 217−227.
(11) Dill, K.; Ghosh, K.; Schmit, J. Physical limits of cells and proteomes. *Proc. Natl. Acad. Sci. U. S. A.* **2011**, *108*, 17876.
(12) Chen, P.; Shakhnovich, E. Thermal adaptation of viruses and bacteria. *Biophys. J.* **2010**, *98*, 1109−1118.
(13) Robertson, A.; Murphy, K. Protein structure and the energetics of protein stability. *Chem. Rev.* **1997**, *97*, 1251−1267.
(14) Ghosh, K.; Dill, K. A. Computing protein stabilities from their chain lengths. *Proc. Natl. Acad. Sci. U. S. A.* **2009**, *106*, 10649−10654.
(15) Sosnick, T. R.; Barrick, D. The folding of single domain proteins: have we reached a consensus? *Curr. Opin. Struct. Biol.* **2011**, *21*, 12−24.
(16) Ghaemmaghami, S.; Oas, T. G. Quantitative proteins stability measurement in vivo. *Nat. Struct. Biol.* **2001**, *8*, 879−882.
(17) Ignatova, Z.; Gierasch, L. M. Monitoring protein stability and aggregation in vivo by real-time fluorescent labeling. *Proc. Natl. Acad. Sci. U. S. A.* **2004**, *101*, 523−528.
(18) McGuffee, S. R.; Elcock, A. H. Diffusion, crowding protein stability in a dynamic molecular model of the bacterial cytoplasm. *PLoS Comput. Biol.* **2010**, *6*, e1000694.
(19) Sarkar, M.; Smith, A. E.; Pielak, G. J. Impact of reconstituted cytosol on protein stability. *Proc. Natl. Acad. Sci. U. S. A.* **2013**, *110*, 19342−19347.
(20) Guo, M.; Xu, Y.; Gruebele, M. Temperature dependence of protein folding kinetics in living cells. *Proc. Natl. Acad. Sci. U. S. A.* **2012**, *109*, 17863−17867.
(21) Kumar, M.; Bava, K.; Gromiha, M.; Parabakaran, P.; Kitajima, K.; Uedaira, H.; Sarai, A. ProTherm and ProNIT: thermodynamic databases for proteins and protein-nucleic acid interactions. *Nucleic Acids Res.* **2006**, *34*, D204−D206.
(22) Ratkowsky, D.; Olley, J.; Ross, T. Unifying temperature effects on the growth rate of bacteria and the ability of globular proteins. *J. Theor. Biol.* **2005**, *233*, 351−362.
(23) Iyer-Biswas, S.; Wright, C.; Henry, J.; Lo, K.; Burov, S.; Lin, Y.; Crooks, G.; Crosson, S.; Dinner, A.; Scherer, N. Scaling laws governing

DOI: 10.1021/acs.jpcb.6b04886
J. Phys. Chem. B 2016, 120, 9549−9563

stochastic growth and division of single bacterial cells. *Proc. Natl. Acad. Sci. U. S. A.* **2014**, *111*, 15912−15917.
(24) Corkrey, R.; Olley, J.; Ratkowsky, D.; McMeekin, T.; Ross, T. Universality of thermodynamic constants governing biological growth rates. *PLoS One* **2012**, *7*, e32003.
(25) Sharma, P.; Xiang, Y.; Kato, M.; Warshel, A. What are the roles of substrate-assisted catalysis and proximity effects in peptide bond formation by the ribosome. *Biochemistry* **2005**, *44*, 11307−11314.
(26) Abbondanzieri, E.; Shaevitz, J.; Block, S. Picocalorimetry of transcription by RNA polymerase. *Biophys. J.* **2005**, *89*, L61−63.
(27) Brunk, E.; Mih, N.; Monk, J.; Zhang, Z.; O'Brien, E.; Bliven, S.; Chen, K.; Chang, R.; Bourne, P.; Palsson, B. Systems biology of the structural proteome. *BMC Syst. Biol.* **2016**, *10*, 26.
(28) Chang, R.; Andrews, K.; Kim, D.; Li, Z.; Godzik, A.; Palsson, B. Structural systems biology evaluation of metabolic thermotolerance in Escherichia coli. *Science* **2013**, *340*, 1220−1223.
(29) Robic, S.; Guzman-Casado, M.; Sanchez-Ruiz, J. M.; Marqusee, S. Role of residual structure in the unfolded state of a thermophilic protein. *Proc. Natl. Acad. Sci. U. S. A.* **2003**, *100*, 11345−11349.
(30) Liu, C. C.; Yang, Y.; LiCata, V. Thermodynamic and structural origins for the extreme stabaility of Taq DNA polymerase. *Biophys. J.* **2009**, *96*, 330a−330a.
(31) Liu, C. C.; Licata, V. J. The stability of Taq DNA polymerase results from a reduced entropic folding penalty; identification of other thremophilic proteins with similar folding thermodynamics. *Proteins: Struct., Funct., Bioinf.* **2014**, *82*, 785−793.
(32) Watanabe, K.; Suzuki, Y. Protein thermostabilization by proline substitutions. *J. Mol. Catal. B: Enzym.* **1998**, *4*, 167−180.
(33) Elcock, A. H. The stability of salt bridges at high temperatures: Implications for hyperthermophilic proteins. *J. Mol. Biol.* **1998**, *284*, 489−502.
(34) Grimsley, G.; Shaw, K.; Fee, L.; Alston, R.; Huyghues-Despointes, B. M. P.; Thurlkill, R.; Scholtz, J.; Pace, C. Increasing protein stability by altering long-range coulombic interactions. *Protein Sci.* **1999**, *8*, 1843−1849.
(35) Loladze, V.; Ibarra-Molero, B.; Sanchez-Ruiz, J.; Makhatadze, G. Engineering a thermostable protein via optimization of charge-charge interactions on the protein surface. *Biochemistry* **1999**, *38*, 16419−16423.
(36) Perl, D.; Mueller, U.; Heinemann, U.; Schmid, F. X. Two exposed amino acid residues confer thermostability on a cold shock protein. *Nat. Struct. Biol.* **2000**, *7*, 380−383.
(37) Clarke, J.; Hounslow, A.; Bond, C.; Fersht, A.; Daggett, V. The effects of disulfide bonds on the denatured state of barnase. *Protein Sci.* **2000**, *9*, 2394−2404.
(38) Kumar, S.; Tsai, C.; Nussinov, R. Factors enhancing protein thermostability. *Protein Eng., Des. Sel.* **2000**, *13*, 179−191.
(39) Pace, C. N.; Alston, R. W.; Shaw, K. L. Charge-charge interactions influence the denatured state ensemble and contribute to protein stability. *Protein Sci.* **2000**, *9*, 1395−1398.
(40) Kumar, S.; Ma, B.; Tsai, C.; Nussinov, R. Electrostatic strengths of salt bridges in thermophilic and mesophilic glutamate dehydrogenase monomers. *Proteins: Struct., Funct., Bioinf.* **2000**, *38*, 368−383.
(41) Dominy, B.; Perl, D.; Schmid, F.; Brooks, C. The effects of ionic strength on protein stability: The cold shock protein family. *J. Mol. Biol.* **2002**, *319*, 541−554.
(42) Loladze, V.; Makhatadze, G. Removal of surface charge-charge interactions from ubiquitin leaves the protein folded and very stable. *Protein Sci.* **2002**, *11*, 174−177.
(43) Kumar, S.; Nussinov, R. Relationship between ion pair geometries and electrostatic strengths in proteins. *Biophys. J.* **2002**, *83*, 1595−1612.
(44) Rosato, V.; Pucello, N.; Giuliano, G. Evidence for cysteine clustering in thermophilic proteomes. *Trends Genet.* **2002**, *18*, 278−281.
(45) Zhou, H. X.; Dong, F. Electrostatic contributions to the stability of a thermophilic cold shock protein. *Biophys. J.* **2003**, *84*, 2216−2222.
(46) Torrez, M.; Schultehenrich, M.; Livesay, D. Conferring thermostability to mesophilic proteins through optimized electrostatic surfaces. *Biophys. J.* **2003**, *85*, 2845−2853.
(47) Alsop, E.; Silver, M.; Livesay, D. R. Optimized electrostatic surfaces parallel increased thermostability: a structural bioinformatic analysis. *Protein Eng., Des. Sel.* **2003**, *16*, 871−874.
(48) Dominy, B.; Minoux, H.; Brooks, C. An electrostatic basis for the stability of thermophilic proteins. *Proteins: Struct., Funct., Bioinf.* **2004**, *57*, 128−141.
(49) Zhou, H. X. Toward the physical basis of thermophilic proteins: Linking of enriched polar interactions and reduced heat capacity of unfolding. *Biophys. J.* **2002**, *83*, 3126−3133.
(50) Cho, J.-H.; Sato, S.; Raleigh, D. Thermodynamics and kinetics of non-native interactions in protein folding: A single point mutant significantly stabilizes the N-terminal domain of L9 by modulating non-native interactions in the denatured state. *J. Mol. Biol.* **2004**, *338*, 827−837.
(51) Berezovsky, I.; Chen, W.; Choi, P.; Shakhnovich, E. Entropic stabilization of proteins and Its proteomic consequences. *PLoS Comput. Biol.* **2005**, *1*, 0322−0332.
(52) Lee, C.; Allen, M.; Bycroft, M.; Wong, K. Electrostatic interactions contribute to reduced heat capacity change of unfolding in a thermophilic ribosomal protein L30e. *J. Mol. Biol.* **2005**, *348*, 419−431.
(53) Huang, X.; Zhou, H. X. Similarity and difference in the unfolding of thermophilic and mesophilic cold shock proteins studied by molecular dynamics simulations. *Biophys. J.* **2006**, *91*, 2451−2463.
(54) Sterpone, F.; Melchionna, S. Thermophilic proteins: insights and perspective from in silicon experiments. *Chem. Soc. Rev.* **2012**, *41*, 1665−1676.
(55) Kalimeri, M.; Rahaman, O.; Melchionna, S.; Sterpone, F. How conformational flexibility stabilizes the hyperthermophilic elongation factor G-domain. *J. Phys. Chem. B* **2013**, *117*, 13775−13785.
(56) Karshikoff, A.; Nilsson, L.; Ladenstein, R. Rigidity versus flexibility: the dilemma of understanding protein thermal stability. *FEBS J.* **2015**, *282*, 3899−917.
(57) Sawle, L.; Ghosh, K. A theoretical method to compute sequence dependent configurational properties in charged polymers and proteins. *J. Chem. Phys.* **2015**, *143*, 085101.
(58) Matthews, B.; Nicholson, H.; Becktel, W. Enhanced protein thermostability from site-directed mutations that decrease the entropy of unfolding. *Proc. Natl. Acad. Sci. U. S. A.* **1987**, *84*, 6663−6667.
(59) Scott, K.; Alonso, D.; Sato, S.; Fersht, A.; Daggett, V. Conformational entropy of alanine versus glycine in protein denatured states. *Proc. Natl. Acad. Sci. U. S. A.* **2007**, *104*, 2661−2666.
(60) Ge, M.; Xia, X.-Y.; Pan, X.-M. Salt bridges in the hyperthermophilic protein Ssh10b are resilient to temperature increases. *J. Biol. Chem.* **2008**, *283*, 31690−31696.
(61) Trevino, S. R.; Schaefer, S.; Scholtz, J. M.; Pace, C. N. Increasing protein conformational stability by optimizing beta-turn sequence. *J. Mol. Biol.* **2007**, *373*, 211−218.
(62) Thompson, M.; Eisenberg, D. Transproteomic evidence of a loop-deletion mechanism for enhancing protein thermostability. *J. Mol. Biol.* **1999**, *290*, 595−604.
(63) Strickler, S.; Gribenko, A.; Gribenko, A.; Keiffer, T.; Tomlinson, J.; Reihle, T.; Loladze, V.; Makhatadze, G. Protein stability and surface electrostatics: a charged relationship. *Biochemistry* **2006**, *45*, 2761−2766.
(64) Robinson-Rechavi, M.; Alibes, A.; Godzik, A. Contribution of electrostatic interactions, compactness and quaternary structure to protein thermostability: Lessons from structural genomics of Thermotoga maritima. *J. Mol. Biol.* **2006**, *356*, 547−557.
(65) Das, R. K.; Pappu, R. V. Conformations of intrinsically disordered proteins are influenced by linear sequence distributions of oppositely charged residues. *Proc. Natl. Acad. Sci. U. S. A.* **2013**, *110*, 13392−13397.
(66) Robinson-Rechavi, M.; Godzik, A. Structural genomics of thermotoga maritime proteins shows that contact order is a major determinant of protein thermostability. *Structure* **2005**, *13*, 857−860.

DOI: 10.1021/acs.jpcb.6b04886
J. Phys. Chem. B 2016, 120, 9549−9563

(67) Fedyukina, D. V.; Jennaro, T. S.; Cavagnero, S. Charge segregation and low hydrophobicity are key features of ribosomal proteins from different organisms. *J. Biol. Chem.* **2014**, *289*, 6740−6750.
(68) Starkereed, P. E.; Oliver, C. N. Protein oxidation and proteolysis during aging and oxidative stress. *Arch. Biochem. Biophys.* **1989**, *275*, 559−567.
(69) Adachi, H.; Fujiwara, Y.; Ishii, N. Effects of oxygen on protein carbonyl and aging in Caenorhabditis elegans mutants with long (age-1) and short (mev-1) life spans. *J. Gerontol., Ser. A* **1998**, *53*, B240−B244.
(70) Sohal, R. S.; Agarwal, S.; Dubey, A.; Orr, W. C. Protein oxidative damage is associated with life expectancy of houseflies. *Proc. Natl. Acad. Sci. U. S. A.* **1993**, *90*, 7255−7259.
(71) Oliver, C. N.; Ahn, B. W.; Moerman, E. J.; Goldstein, S.; Stadtman, E. R. Age-related-changes in oxidized proteins. *J. Biol. Chem.* **1987**, *262*, 5488−5491.
(72) de Graff, A. M. R.; Hazoglou, M. J.; Dill, K. A. Highly charged proteins: the Achilles' heel of aging proteomes. *Structure* **2016**, *24*, 329−336.
(73) Smith, C. D.; Carney, J. M.; Starkereed, P. E.; Oliver, C. N.; Stadtman, E. R.; Floyd, R. A.; Markesbery, W. R. Excess brain protein oxidation and enzyme dysfunction in normal aging and in Alzheimer-disease. *Proc. Natl. Acad. Sci. U. S. A.* **1991**, *88*, 10540−10543.
(74) Stadtman, E. R. Protein oxidation and aging. *Science* **1992**, *257*, 1220−1224.
(75) Stadtman, E. R. Protein oxidation and aging. *Free Radical Res.* **2006**, *40*, 1250−1258.
(76) Davies, K. J. A.; Delsignore, M. E.; Lin, S. W. Protein damage and degradation by oxygen radicals 0.2. Modification of amino-acids. *J. Biol. Chem.* **1987**, *262*, 9902−9907.
(77) Petrov, D.; Zagrovic, B. Microscopic analysis of protein oxidative damage: Effect of carbonylation on structure, dynamics, and aggregability of Villin headpiece. *J. Am. Chem. Soc.* **2011**, *133*, 7016−7024.
(78) Requena, J. R.; Chao, C. C.; Levine, R. L.; Stadtman, E. R. Glutamic and aminoadipic semialdehydes are the main carbonyl products of metal-catalyzed oxidation of proteins. *Proc. Natl. Acad. Sci. U. S. A.* **2001**, *98*, 69−74.
(79) Dill, K. A.; Stigter, D. Modeling protein stability as heteropolymer collapse. *Adv. Protein Chem.* **1995**, *46* (46), 59−104.
(80) Stigter, D.; Alonso, D. O. V.; Dill, K. A. Protein stability - electrostatics and compact denatured states. *Proc. Natl. Acad. Sci. U. S. A.* **1991**, *88*, 4176−4180.
(81) Gitlin, I.; Carbeck, J. D.; Whitesides, G. M. Why are proteins charged? Networks of charge-charge interactions in proteins measured by charge ladders and capillary electrophoresis. *Angew. Chem., Int. Ed.* **2006**, *45*, 3022−3060.
(82) Gudiksen, K. L.; Gitlin, I.; Moustakas, D. T.; Whitesides, G. M. Increasing the net charge and decreasing the hydrophobicity of bovine carbonic anhydrase decreases the rate of denaturation with sodium dodecyl sulfate. *Biophys. J.* **2006**, *91*, 298−310.
(83) Tokuriki, N.; Stricher, F.; Schymkowitz, J.; Serrano, L.; Tawfik, D. S. The stability effects of protein mutations appear to be universally distributed. *J. Mol. Biol.* **2007**, *369*, 1318−1332.
(84) Tacutu, R.; Craig, T.; Budovsky, A.; Wuttke, D.; Lehmann, G.; Taranukha, D.; Costa, J.; Fraifeld, V. E.; de Magalhaes, J. P. Human ageing genomic resources: integrated databases and tools for the biology and genetics of ageing. *Nucleic Acids Res.* **2013**, *41*, D1027−D1033.
(85) Sharma, H. K.; Rothstein, M. Altered enolase in aged Turbatrix-aceti results from conformational-changes in the enzyme. *Proc. Natl. Acad. Sci. U. S. A.* **1980**, *77*, 5865−5868.
(86) Uversky, V. N. Natively unfolded proteins: A point where biology waits for physics. *Protein Sci.* **2002**, *11*, 739−756.
(87) Vidovic, A.; Supek, F.; Nikolic, A.; Krisko, A. Signatures of conformational stability and oxidation resistance in proteomes of pathogenic bacteria. *Cell Rep.* **2014**, *7*, 1393−1400.
(88) Erjavec, N.; Larsson, L.; Grantham, J.; Nystrom, T. Accelerated aging and failure to segregate damaged proteins in Sir2 mutants can be suppressed by overproducing the protein aggregation-remodeling factor Hsp104p. *Genes Dev.* **2007**, *21*, 2410−2421.
(89) Peters, T. W.; Rardin, M. J.; Czerwieniec, G.; Evani, U. S.; Reis-Rodrigues, P.; Lithgow, G. J.; Mooney, S. D.; Gibson, B. W.; Hughes, R. E. Tor1 regulates protein solubility in Saccharomyces cerevisiae. *Mol. Biol. Cell* **2012**, *23*, 4679−4688.
(90) David, D. C.; Ollikainen, N.; Trinidad, J. C.; Cary, M. P.; Burlingame, A. L.; Kenyon, C. Widespread protein aggregation as an inherent part of aging in C. elegans. *PLoS Biol.* **2010**, *8*, e1000450.
(91) Walther, D. M.; Kasturi, P.; Zheng, M.; Pinkert, S.; Vecchi, G.; Ciryam, P.; Morimoto, R. I.; Dobson, C. M.; Vendruscolo, M.; Mann, M.; et al. Widespread proteome remodeling and aggregation in aging C-elegans. *Cell* **2015**, *161*, 919−932.
(92) Ouyang, Z.; Liang, J. Predicting protein folding rates from geometric contact and amino acid sequence. *Protein Sci.* **2008**, *17*, 1256−1263.
(93) Zou, T.; Ozkan, S. Local and non-local native topologies reveal the underlying folding landscape of proteins. *Phys. Biol.* **2011**, *8*, 066011.
(94) Rustad, M.; Ghosh, K. Why and how does native topology dictate the folding speed of a protein? *J. Chem. Phys.* **2012**, *137*, 205104.
(95) Rollins, G.; Dill, K. General mechanism of two-state protein folding kinetics. *J. Am. Chem. Soc.* **2014**, *136*, 11420−11427.
(96) Zou, T.; Williams, N.; Ozkan, S.; Ghosh, K. Proteome folding kinetics is limited by protein halflife. *PLoS One* **2014**, *9*, e112701.
(97) Thirumalai, D. From minimal models to real proteins: time scales for protein folding kinetics. *J. Phys. I* **1995**, *5*, 1457−1467.
(98) Thirumalai, D. Universal relations in the self-assembly of proteins and RNA. *Phys. Biol.* **2014**, *11*, 053005.
(99) Hyeon, C.; Thirumalai, D. Chain length determines the folding rates of RNA. *Biophys. J.* **2012**, *102*, L11−13.
(100) Plaxco, K.; Simons, K.; Baker, D. Contact order, transition state placement and the refolding rates of single domain proteins. *J. Mol. Biol.* **1998**, *277*, 985.
(101) Mashaghi, A.; van Wijk, R.; Tans, S. Circuit Topology of Proteins and Nucleic Acids. *Structure* **2014**, *22*, 1227−1237.
(102) Mugler, A.; Tans, S.; Mashaghi, A. Circuit topology of self-interacting chains: implications for folding and unfolding dynamics. *Phys. Chem. Chem. Phys.* **2014**, *16*, 22537−22544.
(103) Lane, T.; Pande, V. Inferring the rate-length law of protein folding. *PLoS One* **2013**, *8*, e78606.
(104) Belle, A.; Tanay, A.; Bitincka, L.; Shamir, R.; O'Shea, E. Quantification of protein half-lives in the budding yeast proteome. *Proc. Natl. Acad. Sci. U. S. A.* **2006**, *103*, 13004−13009.
(105) Ghosh, K.; Ozkan, S. B.; Dill, K. A. The ultimate speed limit to protein folding is conformational searching. *J. Am. Chem. Soc.* **2007**, *129*, 11920−11927.
(106) Sekhar, A.; Lam, H. N.; Cavagnero, S. Protein folding rates and thermodynamic stability are key determinants for interaction with the Hsp70 chaperone system. *Protein Sci.* **2012**, *21*, 1489−1502.
(107) Reyes-Lamothe, R.; Possoz, C.; Danilova, O.; Sherratt, D. J. Independent positioning and action of Escherichia coli replisomes in live cells. *Cell* **2008**, *133*, 90−102.
(108) Gray, W. J. H.; Midgley, J. E. M. Control of ribonucleic acid synthesis in bacteria - synthesis and stability of ribonucleic acid in rifampicin-inhibited cultures of Escherichia-coli. *Biochem. J.* **1971**, *122*, 161.
(109) Vogel, U.; Jensen, K. F. The RNA chain elongation rate in Escherichia-coli depends on the growth-rate. *J. Bacteriol.* **1994**, *176*, 2807−2813.
(110) Forchhammer, J.; Lindahl, L. Growth rate of polypeptide chains as a function of the cell growth rate in a mutant of Escherichia coli 15. *J. Mol. Biol.* **1971**, *55*, 563−568.
(111) Scott, M.; Gunderson, C. W.; Mateescu, E. M.; Zhang, Z. G.; Hwa, T. Interdependence of Cell Growth and Gene Expression: Origins and Consequences. *Science* **2010**, *330*, 1099−1102.

DOI: 10.1021/acs.jpcb.6b04886
J. Phys. Chem. B 2016, 120, 9549−9563

(112) Liebermeister, W.; Noor, E.; Flamholz, A.; Davidi, D.; Bernhardt, J.; Milo, R. Visual account of protein investment in cellular functions. *Proc. Natl. Acad. Sci. U. S. A.* **2014**, *111*, 8488−8493.
(113) Wittmann, H. G. Components of bacterial-ribosomes. *Annu. Rev. Biochem.* **1982**, *51*, 155−183.
(114) Young, R.; Bremer, H. Polypeptide-chain-elongation rate in Escherichia-coli B-r as a function of growth-rate. *Biochem. J.* **1976**, *160*, 185−194.
(115) Maitra, A.; Dill, K. A. Bacterial growth laws reflect the evolutionary importance of energy efficiency. *Proc. Natl. Acad. Sci. U. S. A.* **2015**, *112*, 406−411.
(116) Karpinets, T. V.; Greenwood, D. J.; Sams, C. E.; Ammons, J. T. RNA: protein ratio of the unicellular organism as a characteristic of phosphorous and nitrogen stoichiometry and of the cellular requirement of ribosomes for protein synthesis. *BMC Biol.* **2006**, *4*, 30.
(117) Verschoor, A.; Warner, J. R.; Srivastava, S.; Grassucci, R. A.; Frank, J. Three-dimensional structure of the yeast ribosome. *Nucleic Acids Res.* **1998**, *26*, 655−661.
(118) Tyson, C. B.; Lord, P. G.; Wheals, A. E. Dependency of size of Saccharomyces-cerevisiae cells on growth-rate. *J. Bacteriol.* **1979**, *138*, 92−98.
(119) Wohlgemuth, I.; Pohl, C.; Mittelstaet, J.; Konevega, A. L.; Rodnina, M. V. Evolutionary optimization of speed and accuracy of decoding on the ribosome. *Philos. Trans. R. Soc., B* **2011**, *366*, 2979−2986.
(120) Johansson, M.; Lovmar, M.; Ehrenberg, M. Rate and accuracy of bacterial protein synthesis revisited. *Curr. Opin. Microbiol.* **2008**, *11*, 141−147.
(121) Klumpp, S.; Scott, M.; Pedersen, S.; Hwa, T. Molecular crowding limits translation and cell growth. *Proc. Natl. Acad. Sci. U. S. A.* **2013**, *110*, 16754−16759.
(122) Bar-Even, A.; Noor, E.; Savir, Y.; Liebermeister, W.; Davidi, D.; Tawfik, D. S.; Milo, R. The moderately efficient enzyme: evolutionary and physicochemical trends shaping enzyme parameters. *Biochemistry* **2011**, *50*, 4402−4410.
(123) Wolf-Watz, M.; Thai, V.; Henzler-Wildman, K.; Hadjipavlou, G.; Eisenmesser, E. Z.; Kern, D. Linkage between dynamics and catalysis in a thermophilic-mesophilic enzyme pair. *Nat. Struct. Mol. Biol.* **2004**, *11*, 945−949.
(124) Kerns, S. J.; Agafonov, R. V.; Cho, Y.-J.; Pontiggia, F.; Otten, R.; Pachov, D. V.; Kutter, S.; Phung, L. A.; Murphy, P. N.; Vu, T.; et al. The energy landscape of adenylate kinase during catalysis. *Nat. Struct. Mol. Biol.* **2015**, *22*, 124−131.
(125) Larion, M.; Hansen, A. L.; Zhang, F.; Bruschweiler-Li, L.; Tugarinov, V.; Miller, B. G.; Brueschweiler, R. Kinetic cooperativity in human pancreatic glucokinase originates from millisecond dynamics of the small domain. *Angew. Chem., Int. Ed.* **2015**, *54*, 8129−8132.
(126) Bahar, I.; Cheng, M. H.; Lee, J. Y.; Kaya, C.; Zhang, S. Structure-encoded global motions and their role in mediating protein-substrate interactions. *Biophys. J.* **2015**, *109*, 1101−1109.
(127) Boehr, D. D.; Dyson, H. J.; Wright, P. E. An NMR perspective on enzyme dynamics. *Chem. Rev.* **2006**, *106*, 3055−3079.
(128) Oyen, D.; Fenwick, R.; Stanfield, R.; Dyson, J.; Wright, P. E. Cofactor-mediated conformational dynamics promote product release from escherichia coli dihydrofolate reductase via an allosteric pathway. *J. Am. Chem. Soc.* **2015**, *137*, 9459−9468.
(129) Guo, J.; Zhou, H.-X. Protein allostery and conformational dynamics. *Chem. Rev.* **2016**, *116*, 6503−6515.
(130) Kumar, A.; Butler, B.; Kumar, S.; Ozkan, S. Integration of structural dynamics and molecular evolution via protein interaction networks: a new era in genomic medicine. *Curr. Opin. Struct. Biol.* **2015**, *35*, 135−142.
(131) Sampedro, J. G.; Uribe, S. Trehalose-enzyme interactions result in structure stabilization and activity inhibition. The role of viscosity. *Mol. Cell. Biochem.* **2004**, *256*, 319−327.
(132) Sampson, N.; Knowles, J. Segmental motion in catalysis: investigation of a hydrogen bond critical for loop closure in the reaction of triosephosphate isomerase. *Biochemistry* **1992**, *31*, 8488−8494.
(133) Mulder, F. A. A.; Mittermaier, A.; Hon, B.; Dahlquist, F. W.; Kay, L. E. Studying excited states of proteins by NMR spectroscopy. *Nat. Struct. Biol.* **2001**, *8*, 932−935.
(134) Rozovsky, S.; Jogl, G.; Tong, L.; McDermott, A. E. Solution-state NMR investigations of triosephosphate isomerase active site loop motion: Ligand release in relation to active site loop dynamics. *J. Mol. Biol.* **2001**, *310*, 271−280.
(135) Wang, L. C.; Pang, Y. X.; Holder, T.; Brender, J. R.; Kurochkin, A. V.; Zuiderweg, E. R. P. Functional dynamics in the active site of the ribonuclease binase. *Proc. Natl. Acad. Sci. U. S. A.* **2001**, *98*, 7684−7689.
(136) Beach, H.; Cole, R.; Gill, M. L.; Loria, J. P. Conservation of mus-ms enzyme motions in the apo- and substrate-mimicked state. *J. Am. Chem. Soc.* **2005**, *127*, 9167−9176.
(137) Eisenmesser, E. Z.; Millet, O.; Labeikovsky, W.; Korzhnev, D. M.; Wolf-Watz, M.; Bosco, D. A.; Skalicky, J. J.; Kay, L. E.; Kern, D. Intrinsic dynamics of an enzyme underlies catalysis. *Nature* **2005**, *438*, 117−121.
(138) Miyashita, O.; Onuchic, J. N.; Wolynes, P. G. Nonlinear elasticity, proteinquakes, and the energy landscapes of functional transitions in proteins. *Proc. Natl. Acad. Sci. U. S. A.* **2003**, *100*, 12570−12575.
(139) Soranno, A.; Buchli, B.; Nettels, D.; Cheng, R.; Muller-Spath, S.; Pfeil, S.; Hoffmann, A.; Lipman, E.; Makarov, D.; Schuler, B. Quantifying internal friction in unfolded and intrinsically disordered proteins with single-molecule spectroscopy. *Proc. Natl. Acad. Sci. U. S. A.* **2012**, *109*, 17800−17806.
(140) Borgia, A.; Wensley, B.; Soranno, A.; Nettels, D.; Borgia, M.; Hoffmann, A.; Pfeil, S.; Lipman, E.; Clarke, J.; Schuler, B. Localizing internal friction along the reaction coordinate of protein folding by combining ensemble and single-molecule fluorescence spectroscopy. *Nat. Commun.* **2012**, *3*, 1195.
(141) Echeverria, I.; Makarov, D.; Papoian, G. Concerted dihedral rotations give rise to internal friction in unfolded proteins. *J. Am. Chem. Soc.* **2014**, *136*, 8708−8713.
(142) de Sancho, D.; Sirur, A.; Best, R. Molecular origins of internal friction effects on protein-folding rates. *Nat. Commun.* **2014**, *5*, 4307.
(143) Klumpp, S.; Scott, M.; Pedersen, S.; Hwa, T. Molecular crowding limits translation and cell growth. *Proc. Natl. Acad. Sci. U. S. A.* **2013**, *110*, 16754−16759.
(144) Kiviet, D.; Nghe, P.; Walker, N.; Boulineau, S.; Sunderlikova, V.; Tans, S. Stochasticity of metabolism and growth at the single-cell level. *Nature* **2014**, *514*, 376−379.
(145) Tokuyama, M.; Oppenheim, I. On the theory of concentrated hard-sphere suspensions. *Phys. A* **1995**, *216*, 85−119.
(146) Schmit, J.; Kamber, E.; Kondev, J. Lattice model of diffusion-limited bimolecular chemical reactions in confined environments. *Phys. Rev. Lett.* **2009**, *102*, 218302.
(147) Konopka, M.; Sochacki, K.; Bratton, B.; Shkel, I.; Record, M.; Weisshaar, J. Cytoplasmic protein mobility in osmotically stressed escherichia coli. *J. Bacteriol.* **2009**, *191*, 231−237.
(148) Muramatsu, N.; Minton, A. Tracer diffusion of globular proteins in concentrated protein solutions. *Proc. Natl. Acad. Sci. U. S. A.* **1988**, *85*, 2984−2988.
(149) Tan, C.; Saurabh, S.; Bruchez, M.; Schwartz, R.; LeDuc, P. Molecular crowding shapes gene expression in synthetic cellular nanosystems. *Nat. Nanotechnol.* **2013**, *8*, 602−608.
(150) Nunes, P.; Roth, I.; Meda, P.; Feraille, E.; Brown, D.; Hasler, U. Ionic imbalance, in addition to molecular crowding, abates cytoskeletal dynamics and vesicle motility during hypertonic stress. *Proc. Natl. Acad. Sci. U. S. A.* **2015**, *112*, E3104−3113.
(151) Mourao, M. A.; Hakim, J. B.; Schnell, S. Connecting the Dots: The fffects of macromolecular crowding on cell physiology. *Biophys. J.* **2014**, *107*, 2761−2766.
(152) Matsuda, H.; Putzel, G.; Backman, V.; Szleifer, I. Macromolecular crowding as a regulator of gene transcription. *Biophys. J.* **2014**, *106*, 1801−1810.
(153) Miermont, A.; Waharte, F.; Hu, S.; McClean, M. N.; Bottani, S.; Leon, S.; Hersen, P. Severe osmotic compression triggers a

DOI: 10.1021/acs.jpcb.6b04886
J. Phys. Chem. B 2016, 120, 9549−9563

slowdown of intracellular signaling, which can be explained by molecular crowding. *Proc. Natl. Acad. Sci. U. S. A.* **2013**, *110*, 5725−5730.
(154) Parry, B. R.; Surovtsev, I. V.; Cabeen, M. T.; O'Hern, C. S.; Dufresne, R.; Jacobs-Wagner, C. The bacterial cytoplasm has glass-like properties and is fluidized by metabolic activity. *Cell* **2014**, *156*, 183−194.

DOI: 10.1021/acs.jpcb.6b04886
J. Phys. Chem. B 2016, 120, 9549−9563